



HAL
open science

CeO₂-based peelable gel for neutralization and skin decontamination toward chemical warfare agents

Eloise Thomas, Claire Bordes, Frédéric Chaput, Delphine Arquier, Stéphanie Briançon, Marie-Alexandrine Bolzinger

► **To cite this version:**

Eloise Thomas, Claire Bordes, Frédéric Chaput, Delphine Arquier, Stéphanie Briançon, et al.. CeO₂-based peelable gel for neutralization and skin decontamination toward chemical warfare agents. *Colloids and Surfaces A: Physicochemical and Engineering Aspects*, 2024, 687, pp.133520. 10.1016/j.colsurfa.2024.133520 . hal-04480655

HAL Id: hal-04480655

<https://hal.science/hal-04480655v1>

Submitted on 19 Nov 2024

HAL is a multi-disciplinary open access archive for the deposit and dissemination of scientific research documents, whether they are published or not. The documents may come from teaching and research institutions in France or abroad, or from public or private research centers.

L'archive ouverte pluridisciplinaire **HAL**, est destinée au dépôt et à la diffusion de documents scientifiques de niveau recherche, publiés ou non, émanant des établissements d'enseignement et de recherche français ou étrangers, des laboratoires publics ou privés.

1 **CeO₂-based peelable gel for neutralization and skin**

2 **decontamination toward chemical warfare agents**

3
4 Eloise Thomas* ^{a,b}, Claire Bordes^a, Frédéric Chaput^c, Delphine Arquier^b, Stéphanie Briançon ^{a,b}, Marie-
5 Alexandrine Bolzinger ^{a,b}

6
7 ^a Université Claude Bernard Lyon 1, UMR5007 CNRS, LAGEPP, 43 boulevard du 11 novembre 1918,
8 Bâtiment CPE, 69622, Villeurbanne Cedex, France. eloise.thomas@univ-lyon1.fr, [claire.bordes@univ-](mailto:claire.bordes@univ-lyon1.fr)
9 [lyon1.fr](mailto:delphine.arquier@univ-lyon1.fr), delphine.arquier@univ-lyon1.fr, stephanie.briancon@univ-lyon1.fr, [lyon1.fr](mailto:marie.bolzinger@univ-
10 <a href=)

11 ^b Institut des Sciences Pharmaceutiques et Biologiques, Laboratoire de Dermopharmacie et
12 Cosmétologie, Université Claude Bernard Lyon 1, 69008, Lyon, France. eloise.thomas@univ-lyon1.fr,
13 delphine.arquier@univ-lyon1.fr, stephanie.briancon@univ-lyon1.fr, marie.bolzinger@univ-lyon1.fr

14 ^c École Normale Supérieure de Lyon, Université Claude Bernard Lyon 1, CNRS UMR 5182, Laboratoire
15 de Chimie, 46 allée d'Italie, 69364, Lyon, France. frederic.chaput@ens-lyon.fr

16
17 * Corresponding author: Eloise Thomas, eloise.thomas@univ-lyon1.fr

18

19 ABSTRACT

20 Accidents with toxic industrial chemicals and threats posed by chemical warfare agents, as
21 organophosphorus nerve agents and blistering agents, has become an increasing concern over the last
22 decades. Intoxication is not only due to inhalation but dermal route can also be important and can
23 quickly lead to death. It is therefore crucial to have suitable means of personal protection and
24 decontamination. Some are already commercially available but often present drawbacks. Efforts have
25 been made to develop new systems and several studies have shown the interest of metallic
26 nanoparticles. The challenge remains to entrap the particles in an adapted matrix to limit their
27 diffusion in the immediate environment, while preserving the bare particles decontamination efficacy.
28 In this study, an easy to handle peelable gel, incorporating CeO₂ nanoparticles has been developed for
29 efficient skin decontamination against toxic chemicals. The main objective has been to render it
30 suitable in any context of application (battlefield or civil exposure). Nano-octahedra (NO) CeO₂
31 particles synthesized in this study have been able to increase the degradation of paraoxon, a simulant
32 warfare agent in liquid media. NO have then been incorporated in a peelable gel, the formulation has
33 been optimized through design of experiments and its physico-chemical properties characterized. Even
34 after incorporation to the gel, NO retained their neutralization properties. The formulation efficiency
35 towards neutralization and skin decontamination have been evaluated *in vitro* on Franz diffusion cells.
36 The interest of the peelable gel have been clearly demonstrated with a decrease by about 5-fold of the
37 quantity of POX absorbed into the skin and a decrease of 3 to 4-fold in the viable skin, which was much
38 higher than the use of cotton or nanoparticles as powder.

39 KEY WORDS

40 Cerium dioxide nanoparticle - Peelable gel – Skin decontamination – Paraoxon

41 1 INTRODUCTION

42 In an international context strongly marked since 2013 by the use of chemical weapons, in war or
43 terrorist attacks [1], the development of effective countermeasures against organophosphorus nerve
44 agents - OPs (VX, sarin, soman, tabun) and blistering agents (organochlorines - OCs) such as sulphur
45 mustard appears essential both for battlefield or civil situation [2]. Intoxication is not only due to
46 inhalation but dermal route can also be important and can quickly lead to death [2]. VX is the best
47 known and most widely used of OPs because of its very low volatility and high toxicity which is
48 explained by the presence of a P=O bond. This bond inhibits the enzyme acetylcholinesterase (AChE),
49 an essential enzyme in the transmission of nerve signals, [1], [2], [3]. The oily appearance and lipophilic
50 nature of VX allows it to penetrate the skin and, a single drop can cause death very quickly. It is
51 therefore crucial to have the appropriate personal protection and decontamination equipment [4].
52 The objective of decontamination is to eliminate and ideally to degrade the chemical substances
53 present on the victim's skin surface, clothing or surrounding surfaces in a very short time in order to
54 limit intoxication and contamination transfer. The ideal decontamination systems should be effective
55 on a wide spectrum of chemicals, easy to handle and prevent subsequent recontamination.

56 Different decontamination systems have been proposed and vary according to the nature of the
57 materials used, their form (solid, liquid,...), their mechanism of action (displacement/adsorption of the
58 toxicant or degradation into safer by-products), etc. [5]. Washing the skin with water or soap and water
59 is probably the simplest and least expensive decontamination strategy. It neutralizes the contaminant
60 by dilution and sometimes by partial hydrolysis. However, recent studies have shown that these
61 methods often result in incomplete decontamination [6] and, may also elicit contaminant absorption
62 due to the "wash-in" effect [7], [8]. Indeed, water associated or not to soapy solutions or chemicals is
63 known to be a conventional enhancer that may increase skin permeability of molecules probably due
64 to the temporary skin hydration leading to a reduction in skin barrier properties [9]. Zhu et al. [10]
65 have recently shown that the penetration of benzoic acid and paraoxon into the stratum corneum

66 increased with the stratum corneum hydration levels. Other drawbacks of such strategy are the need
67 of large volumes of water and the fact that they do not fully degrade the toxicant. Therefore, it
68 generates large quantities of toxic waste and increases secondary contamination risks [6], [7]. Fuller's
69 earth has been frequently used as decontaminant. This safe powder is an effective adsorbent for
70 various chemicals as VX and mustard gas and has been shown to reduce their penetration into the
71 skin [11], [12], [13], [14]. Fuller earth leads to a rapid decontamination, is inexpensive and stable over
72 time. However, the powder is relatively volatile and inhalation of contaminated powder remains a risk.
73 To overcome this drawback, a glove retaining the powder can be used. Nevertheless, Fuller's earth
74 does not degrade toxics once absorbed at its surface, which increases the risk of cross contamination
75 [11], [12], [13], [14]. Decontamination systems able to degrade the toxics into safer by products exist
76 as the Reactive Skin Decontamination Lotion (RSDL), which is the most widely used liquid
77 decontaminant for skin. It is currently considered as a standard decontamination lotion as such or
78 soaked in a sponge for easier application [4], [11], [15], [16], [17], [18]. However, the product cannot
79 be applied on wounds and eyes, is relatively expensive and not very stable over time.

80 In the context of the development of new effective strategies for skin decontamination, research has
81 focused on systems inexpensive and easy to handle, able to displace and degrade toxic compounds, to
82 prevent any spread and to facilitate waste treatment. Several studies have shown the interest of metal
83 oxides (TiO_2 , MgO , ZnO , Al_2O_3 ...) [19], [20], [21], [22], [23], [24] for adsorption and neutralization of
84 chemicals into safer by-products. For example, we have previously synthesized ceria (CeO_2)
85 nanoparticles and demonstrated *in vitro* their interests for the degradation of paraoxon (POX), a
86 pesticide and model for OPs, in aqueous solution [25], [26], [27], [28]. *In vitro* experiment performed
87 with Franz cells have also showed that CeO_2 suspensions and RSDL were the most efficient to remove
88 POX from the skin surface and decrease skin absorption compared to the control (not decontaminated
89 skin) [27]. Other studies have focused on the use of ceria for the degradation of various chemicals as
90 VX, Soman or sulfur mustard [27], [29], [30], [31] demonstrating its interest in this context. CeO_2
91 nanoparticles have found application in the field of biomedicine owing to their low toxicity. They have

92 demonstrated good tolerance in both *in vitro* and *in vivo* biological models, as indicated by Das et al.
93 [32]. This favorable profile supports their potential use in skin decontamination systems. However, it
94 is crucial to thoroughly investigate the safety of ceria particles upon skin application, as it can
95 significantly impact their practical application. Forest et al. conducted an *in vitro* study on macrophages
96 from the RAW264.7 cell line to explore the impact of ceria nanoparticles [33]. The results revealed no
97 reactive oxygen species (ROS) production, but there was a dose-dependent increase in LDH release
98 and TNF- α production with rod-like nanoparticles, while no variation was observed with
99 cubic/octahedral nanoparticles. Hence, the nanoparticle shape plays a pivotal role and must be
100 carefully considered in the development of CeO₂-based skin decontaminant systems. In our study, we
101 specifically chose nano-octahedra particles (NO). Additionally, the penetration of nanoparticles into
102 the skin is a critical parameter. Generally, nanoparticle penetration is strongly influenced by their size.
103 Nanoparticles with a size below 4 nm can penetrate and permeate intact skin, those between 4 and
104 20 nm can potentially permeate intact and damaged skin, and those between 21 and 45 nm can
105 penetrate and permeate only damaged skin. Nanoparticles larger than 45 nm cannot penetrate or
106 permeate the skin [34]. To prevent the penetration of CeO₂ nanoparticles into the skin, larger sizes
107 may be employed, or nanoparticles can be entrapped in a matrix to hinder their penetration. This
108 strategic approach is the focus of our current study.

109 Most of the time, metal oxides are used as powder but extremely fine powders should be avoided to
110 limit dispersal and possible inhalation and pulmonary effects. The technological issue is therefore to
111 entrap metal oxide particles in a system able to limit their diffusion in the immediate environment,
112 while preserving the bare particles decontamination efficacy. Only few solutions have been proposed
113 so far. Systems with metal oxide particles adsorbed onto tissues have been designed. For example,
114 ZnTiO₃ and AgNO₃ have been incorporated into polyester wipes and their efficiency evaluated on
115 diethylchlorophosphate and sulfur mustard simulants [35]. Metal oxides have also been embedded in
116 gloves as Fast-act, a glove combining titanium dioxide (TiO₂) and magnesium oxide (MgO), and efficient
117 against various chemicals [12], [13]. Only few other studies have focused on other type of formulations

118 such as metal oxide incorporated into a cream [36], [37], [38] or suspension of Fe₃O₄ grafted onto
119 polymers [39]. However these formulations were either used as skin protectant and not as
120 decontaminant ([36], [37], [38]) or their skin efficiency has not been studied [39]. In this context, the
121 objective of this study was to develop an innovative CeO₂-based formulation for efficient skin
122 decontamination against toxic chemicals. Our scientific investigation presents several distinctive
123 features that differentiate it from prior research. The formulation designed here: 1) allows absorption
124 and degradation of the toxic agent, and limits waste (on the contrary to the use of water or Fuller's
125 Earth) ; 2) enables easy application and removal; it is adapted to the context of application, battlefield
126 or civil exposure (unlike volatile powders or solutions requiring a sponge) ; 3) limits the amount of
127 water to avoid a wash-in effect; 4) allows its use on damaged skin (unlike RSDL). A peel-off gel
128 incorporating CeO₂ nanoparticles in its network has been developed. It has continuous thick
129 consistency and can be applied on the skin. It is allowed to dry in few minutes and then it is peeled off.
130 The framework of our study includes nanoparticles synthesis and characterization, formulation and a
131 thorough understanding of interactions and optimization through design of experiment. Finally, the
132 formulation has been optimized and its properties characterized. Its efficiency towards neutralization
133 and skin decontamination of a simulant warfare agent (paraoxon, POX) has been evaluated *in vitro* on
134 Franz diffusion cells.

135 2 MATERIAL & METHODS

136 2.1 MATERIALS

137 Cerium nitrate hexahydrate Ce(NO₃)₃·6H₂O (99.5%) was purchased from Alfa Aesar and ammonium
138 hydroxide NH₄OH (ACS grade) from Carlo Erba. POX (O,O-diethyl p-nitrophenyl phosphate, purity 90%)
139 was purchased from Sigma. Ethanol (96.3%) and P-nitrophenol (PNP, 99% purity) from Acros Organics
140 Company, methanol and glacial acetic acid (HPLC grade) were purchased from Fisher Scientific.
141 Kollidon® SR (physical mixture of 80% polyvinyl acetate + 19% povidone, Kollidon® 30) and Lutrol F127

142 (polyoxypropylene-polyoxyethylene block copolymer or poloxamer 407) were a gifted by BASF. Klucel
143 HF Pharm (hydroxypropyl cellulose, HPC, MW= 1 150 kDa), Klucel EF Pharm (HPC, MW = 80 kDa) were
144 a kind gift from Ashland. Cekol 30 000 (carboxymethyl cellulose, CMC, MW = 750 kDa) were gifted from
145 Cp Celco. Carboxymethyl cellulose (CMC, MW = 90 kDa) were purchased from Acros Organics.
146 Ultrapure water (resistivity > 18 MΩ.cm) was used for formulation and analysis. All chemicals were
147 obtained and used without further purification.

148 2.2 METHODS

149 2.2.1 Nano-octahedra (NO) CeO₂ particles synthesis and characterization

150 The nanoparticles synthesis was performed by hydrothermal process as described in the literature
151 [26]. Briefly, 0.0255 mol of Ce(NO₃)₃·6H₂O was dissolved in 20 mL of distilled water. This solution was
152 added to a 130 mL solution containing 0.102 mol of ammonium hydroxide NH₄OH at room temperature
153 under strong stirring. After stirring for 20 min, the solution was transferred into a Teflon-lined stainless-
154 steel autoclave and heated at 180 °C (10.5 bars) for 24 hours. After hydrothermal treatment and
155 autoclave cooling, the precipitate present in the reaction medium was then recovered by
156 centrifugation, washed four times with distilled water and dried in an oven at 60°C for 10 hours in
157 ambient air. 4.4 g of nano-octahedra powder were obtained for 11.1 g of cerium nitrate hexahydrate
158 used (one batch, about 100% yield). A heat treatment was then carried out at 500°C for 2 hours. The
159 NO obtained were characterized by transmission electron microscopy (TEM) to evaluate the size and
160 shape of the nanoparticles, by the gas adsorption technique (BET) for the determination of the specific
161 surface area and by X-ray diffraction to lattice parameters and crystallite size determination. The
162 particles were observed by transmission electron microscopy (TEM) using a JEOL 2100 HT operating at
163 200 kV. High-resolution transmission electron microscopy (HRTEM) images were also performed. The
164 TEM samples were prepared by drop-casting the suspension onto TEM grids. The size of the
165 nanoparticles was determined from TEM images by counting 100 particles according to the procedure
166 described by Trenque et al. [25]. The specific surface area of the as-prepared samples was calculated

167 from the adsorption/desorption isotherms of nitrogen at 77 K using a BELSORP-max instrument (Passy,
168 France). The Brunauer–Emmett-Teller (BET) method was used for surface area calculation. X-ray
169 diffraction (XRD) patterns were recorded on a Bruker D8 Advance diffractometer equipped with a
170 sealed Cu X-ray tube (40 kV, 40 mA) and a linear Lynxeye XE detector. Data were collected over the
171 range 5–90° with 0.0205° step size. The lattice parameters and the crystallite sizes were extracted from
172 XRD patterns by profile matching (LeBail fit) using the elementary pseudo-Voigt function with the
173 FullProf program packages.

174 2.2.2 POX degradation in solution

175 The *in vitro* degradation of POX and study of the apparition of PNP was performed (n=3-5). Suspension
176 of NO in water (pH=7) or EtOH were prepared and temperature adjusted at 32°C. At t=0, a solution of
177 POX was added to NO suspension to reach a POX concentration of 0.055 g.L⁻¹ (200 mg NO, 2 mL).
178 Suspension were stirred at 37°C for 5 h. At different time point of contact between POX and NO,
179 supernatant was collected, diluted by 10 in water, filtrated on 0.2 µm to remove NO and analyzed by
180 HPLC. A one-order kinetic model has been used to fit the data [28]. A POX solution without NO was
181 taken as control.

182 2.2.3 Quantification of POX and PNP by HPLC

183 POX and PNP were analyzed from samples using high-pressure liquid chromatography equipped with
184 a XTerra® MS-C18 column (5 µm, 4.6 mm×250 mm) as already described [25], [27]. An HPLC
185 Waters Alliance 2695 coupled with a 2998 photodiode array detector (PDA), working at 269 and
186 314 nm wavelength, was used. The column oven temperature was maintained at 40°C. The calibration
187 curve was prepared between 0 and 100 µg/mL. The elution of 10 µL of the samples with
188 methanol/water (acidified with 0.5% (v/v) acetic acid) at a flow rate of 0.7 mL.min⁻¹ gave a retention
189 time of 7.5 min for POX and 5.5 min for PNP. For all experiments, samples were always filtrated on
190 0.45 µm membrane disc filter before injection.

191 2.2.4 Peelable gel formulation

192 2.2.4.1 *Choice of raw materials*

193 A peel-off gel is a topical product that dries to form an occlusive film layer that can be peeled off after
194 application. Peel-off gel contains film-forming and gelling agents. The gel must have good skin adhesive
195 properties, a shear thinning behavior and, a short drying time. It must stay flexible even after the drying
196 process. In this part, different tests were carried out to select raw materials giving a final product with
197 appropriate properties for use as a skin decontamination product. Various cellulose derivatives were
198 selected and tested at different molecular weights as gelling agents for their mucoadhesive properties
199 and because they provide high viscosities (carboxymethyl cellulose CMC, hydroxypropyl cellulose HPC).
200 Different film-forming agents were also tested: Kollidon® SR (mixture of 80% of polyvinyl acetate and
201 19% povidone), pure PVP, PVP-hexadecene copolymer and PVP-eicosene copolymer. Finally, different
202 amount of NO particles synthesized as reported in 3.2.1 were added.

203 A typical formulation procedure was as following: the solvents were mixed with a deflocculating stirrer
204 at 300 rpm (Rayneri VMI) (10 mL ethanol and 2 mL water). Kollidon® SR (3 g), poloxamer 407 (1 g),
205 carboxymethyl cellulose (0.3 g) were added progressively parts by parts under stirring. The mixture
206 was then covered with an aluminum foil to avoid solvent evaporation. Then, the NO particles (1 g)
207 were gradually dispersed in the gel and the stirring process was continued for 4 h to ensure a
208 homogenous dispersion. Gels were stored in an airtight bottle.

209 All formulations were characterized before drying in order to determine their properties in terms of
210 texture, stability, and drying time as described below in part 2.2.5. The texture analyzer measurements
211 and rheology studies were performed to link sensory parameters and physicochemical properties.

212 2.2.4.2 *Design of experiment*

213 The formulation was optimized by using a 2^{k-1} fractional factorial design where k represents the
214 number of experimental factors to study (k=5), each at two levels [40]. The chosen experimental
215 domain or compounds used in the design of experiments (DOE) were selected according to the

216 preliminary tests. The variable experimental factors with their two levels and the fixed parameters are
 217 reported in Table 1.

218 *Table 1: Fixed and variable factors used for the experimental design.*

Variable parameters		
Coded level	(-1)	(+1)
Kollidon® SR quantity (X ₁)	2 g	3 g
Poloxamer 407 quantity (X ₂)	0.5 g	1.5 g
Type of thickening agent (X ₃)	HPC MW = 1 150 kDa (Klucel HF)	HPC MW = 80 kDa (Klucel EF)
Quantity of thickening agent (X ₄)	0.3 g	0.8 g
Ratio EtOH/Water (X ₅)	80/20	99/1
Fixed parameters		
Nanoparticles quantity	1 g	
Total solvent	9.89 g	

219

220 The 16 runs defined by the experimental design are described in the Table 2. The DOE objective was
 221 to improve the formulation of the gel regarding its use on skin. Results of the different
 222 characterizations are presented in the Supplementary Information (Table S1).

223 *Table 2: Formulations prepared according to a 2⁵⁻¹ fractional factorial design.*

N°Exp	Kollidon® SR (g)	Poloxamer 407 (g)	Type of thickening agent	Quantity of thickening agent (g)	Ratio EtOH/Water
F1	2	0.5	HPC 1 150 kDa	0.3	99/1
F2	3	0.5	HPC 1 150 kDa	0.3	80/20
F3	2	1.5	HPC 1 150 kDa	0.3	80/20
F4	3	1.5	HPC 1 150 kDa	0.3	99/1
F5	2	0.5	HPC 80 kDa	0.3	80/20
F6	3	0.5	HPC 80 kDa	0.3	99/1
F7	2	1.5	HPC 80 kDa	0.3	99/1
F8	3	1.5	HPC 80 kDa	0.3	80/20
F9	2	0.5	HPC 1 150 kDa	0.8	80/20
F10	3	0.5	HPC 1 150 kDa	0.8	99/1
F11	2	1.5	HPC 1 150 kDa	0.8	99/1
F12	3	1.5	HPC 1 150 kDa	0.8	80/20
F13	2	0.5	HPC 80 kDa	0.8	99/1
F14	3	0.5	HPC 80 kDa	0.8	80/20
F15	2	1.5	HPC 80 kDa	0.8	80/20

224

225 The use of such DOE consists in approximating the experimental gel characteristics to be improved (Y_i)
226 by a two-factor factorial model written as:

$$227 \quad \hat{Y}_i = b_0 + \sum_{i=1}^5 b_i X_i + \sum_{i,j=1}^5 b_{ij} X_i X_j \quad (1)$$

228 where \hat{Y}_i is the predicted response (with gel hardness (Y_1), relaxation (Y_2), stickiness (Y_3), stability score
229 (Y_4)), b_0 is the intercept, the coefficient b_i is the main effect of the coded factor X_i and the coefficients
230 b_{ij} are the two-factors interaction effects. The coefficients of Eq. (1) were determined for each
231 response by ordinary least square regression. Multiple linear regression analyses were performed
232 using NemrodW[®] software (LPRAI, Marseille, France).

233

234 2.2.5 Peelable gel characterizations

235 2.2.5.1 *Characterization of the gel, before drying*

236 Stability of the formulations was evaluated by keeping the gel in an air-tight vial at room temperature
237 or 45°C for 6 months and checking for any visual change in the formulation (sedimentation, gel
238 syneresis). A score from 0 to 10 was then given to rank the formulations according to their stability, 10
239 corresponding to the most stable formulations (no change detected) and 0 to the less stable
240 formulations (sedimentation of gel syneresis detected after preparation and no return to an
241 homogeneous suspension after manual mixing for 30 s). The texture analyzer was used to determine
242 the hardness, elasticity and stickiness of the gels and to link sensory parameters to physicochemical
243 properties in order to optimize the formulation. Different parameters (choice of probe, probe
244 approach and return speed, probe insertion distance and relaxation time) were optimized in order to
245 obtain repeatable results. Characterizations of the gels were performed with the TX-700 texture
246 analyzer (LAMY Rheology) using a flat probe ($d = 4$ cm) and an extrusion cell. Parameters for the

247 compression and relaxation study were: speed: 1.5 mm/s, depth: 5 mm and relaxation time: 30 s. For
248 the traction study, parameters were: manual approach at the gel surface, 60 s relaxation before
249 traction, traction speed: 0.5 mm/s. According to preliminary tests, a satisfactory texture should have
250 hardness values around 5 N, stickiness close to 0 N and a percentage of relaxation (which is inversely
251 proportional to the elasticity of the product) above 90%. The film drying process was evaluated by
252 spreading the gels on glass slides and on membranes (Strat-M® membranes, Milipore) as interactions
253 were different for glass or membrane and placing them at 32°C to mimic the skin surface temperature.
254 The film drying was observed until detachment of the glass side or membrane was possible.

255 2.2.5.2 *Characterization of the film obtained after drying*

256 The flexibility of the films obtained after drying of the peelable gel was characterized with the TX-700
257 texture analyzer (LAMY Rheology) using a film compression bench and a compression method with a
258 probe insertion of 20 cm in the film. Images of the films as well as a mapping of the cerium atoms were
259 obtained by using a Scanning Electron Microscope (FEI Quanta 250 FEG) with copper or carbon
260 metallization (deposition = 10 nm) and an acceleration voltage of 10 kV coupled with energy dispersive
261 X-ray spectroscopy (EDX).

262 2.2.6 Degradation of POX by peelable gel

263 POX (25.4 µL) was gently mixed in the formulation F2 (prepared with and without NO particles, 0.5 g).
264 After 30 min at room temperature, 40 mL of EtOH was added, and the solution was vortexed for 1 min
265 to extract POX from the formulation. Solution was then diluted in EtOH, filtrated on 0.45 µm nylon
266 membrane disc filter and analyzed with HPLC. Experiment was performed in triplicate. Results are
267 reported as mean ± SD.

268 2.2.7 Evaluation of skin decontamination efficiency

269 Pig-ears were collected immediately after animals were killed (Ecole de Chirurgie, University Lyon 1,
270 France). They were stored flat at -20°C for a maximum period of 6 months. The skin was prepared
271 following the procedure described in litterature [41]. 5 replicates for each decontamination systems

272 were performed. On the day of the experiment, the skin samples (1.2 ± 0.1 mm thick) were thawed
273 and mounted on Franz-type static glass diffusion cells with a surface area of 2.54 cm^2 . Ultrapure water
274 was used as acceptor medium. The cells were maintained at 37°C in a water bath in order to reach the
275 *in vivo* skin surface temperature of $32 \pm 1^\circ\text{C}$. Skin integrity was assessed by measuring the
276 transepidermal water loss (Tewameter TM300, Courage & Khazaka). Only skin explants with
277 transepidermal water loss values ranging between 3 and $10. \text{g} \cdot \text{h}^{-1} \cdot \text{m}^{-1}$ were used in the penetration
278 studies.

279 For decontamination study, $25.4 \mu\text{L}$ of pure POX divided into microdroplets were applied on the pig-
280 ear skin surface in the donor compartment of the cell. This resulted in an applied dose of
281 $Q_0 = 13 \text{ mg}/\text{cm}^2$ (or $10 \mu\text{L}/\text{cm}^2$ or $46 \mu\text{mol}/\text{cm}^2$) and corresponds to a full coverage of the skin. The
282 solubility of POX in the acceptor medium ($2.4 \text{ mg}/\text{mL}$ at 25°C) ensured that sink conditions were
283 applied since the highest POX concentration in the acceptor medium after the series of experiment
284 was $5 \mu\text{g}/\text{mL}$. Consequently, it was not a rate-limiting step in skin absorption. After 30 minutes of
285 exposure to the toxic, the skin was decontaminated by applying the different decontamination
286 systems: peelable gel containing NO particles, peelable gel without NO particles, NO particles as
287 powder and cotton only. Some skin samples were not decontaminated and are referred as control in
288 the following. The course of experiment was 24h.

289 For gel (containing NO or not), 0.5 g of gel was deposited which corresponds to 34 mg of NO. This
290 quantity of gel leads to a total coverage of the skin surface, while maintaining a correct thickness. This
291 corresponds to the use of the system in real-life conditions. Gel was massaged on the surface in a
292 circular motion on each skin disc for 20 seconds with a cotton swab covered with part of a glove to
293 mimic a manual application. The cotton swab and glove were then added to 20 mL EtOH for POX
294 extraction and HPLC analysis. 60 min after the contamination (ie 30 min after application of the
295 decontamination systems), gels were removed and added to 20 mL EtOH for POX extraction and HPLC
296 analysis. The skin surface was then gently wiped with 3 cotton balls (2 slightly damp and one dry) to

297 remove the last residues of gels. Cottons were then added to 20 mL EtOH for POX extraction and HPLC
298 analysis. Simulants permeation assay was continued for 24 hours to ascertain the impact of the skin
299 decontamination process on dermal penetration and percutaneous absorption. For decontamination
300 with the NO particles powder, the same protocol was followed but 34 mg of NO were directly
301 deposited by sprinkling the entire surface with the powder. Tests were also performed following the
302 same protocol but without addition of gel or powder (samples are called cotton in the following).
303 Finally, some skin samples were not decontaminated and are referred as control in the following
304 (n = 5).

305 24 h after POX exposure, skin surface was washed 3 times with 3 mL of distilled water and dried with
306 absorbing paper. The three washings and absorbing papers were each added to 17 mL EtOH, filtered
307 and analyzed by HPLC analysis. Then the acceptor medium was collected. Skin samples were removed
308 from the diffusion cells. The first strip S1 was quickly removed using D-Squame tape (Monaderm) and
309 placed in a vial with 3 mL of EtOH. S1, the washing water and absorbing papers at 24 h represent the
310 POX remaining on the surface of the skin after decontamination and is called surface (S) in the rest of
311 the article. The stratum corneum was separated from the viable epidermis and dermis using the
312 stripping method and, stripes were pooled three by three and placed in different vials each containing
313 3 mL of ethanol (12 strips were used during this step). Then, the viable epidermis (E) was separated
314 from the dermis by heat treatment (45 s in water at 60 °C), cut into small pieces and deposited in a vial
315 containing 2 mL of ethanol. The vials were placed for 2h under magnetic stirring at room temperature
316 to extract POX. The dermis (D) was cut into small pieces and placed in a vial filled with ethanol. It was
317 extracted 4 times under magnetic stirring at room temperature, 1 time with 4 mL EtOH and 3 times
318 with 2 mL EtOH. After each extraction, aliquots were diluted if needed and filtered on a nylon
319 membrane disc filter (0.45 µm pore-size, 25 mm diameter) before HPLC quantification. It was verified
320 that this protocol led to a 100 % recovery of POX. The 100% recovery was verified on samples not
321 decontaminated at all, samples decontaminated with cotton only and samples decontaminated with
322 gel not containing NO particles (ie: all the decontamination systems which don't involve a chemical

323 degradation of the POX). In all cases, the total POX recovered from all the fractions was above 85% of
324 the initial dose deposited.

325 The mean and standard error (SD) of n = 5 determinations were calculated. Statistical comparisons
326 were made using nonparametric test of Mann-Whitney (with the two-sided level of significance $\alpha =$
327 0.05).

328 Three ratios were calculated to compare the different decontaminant systems with the control (no
329 decontamination):

$$330 \quad \text{Ratio} = \frac{\% \text{ of POX for the control}}{\% \text{ of POX for the decontaminant system}} \quad (2)$$

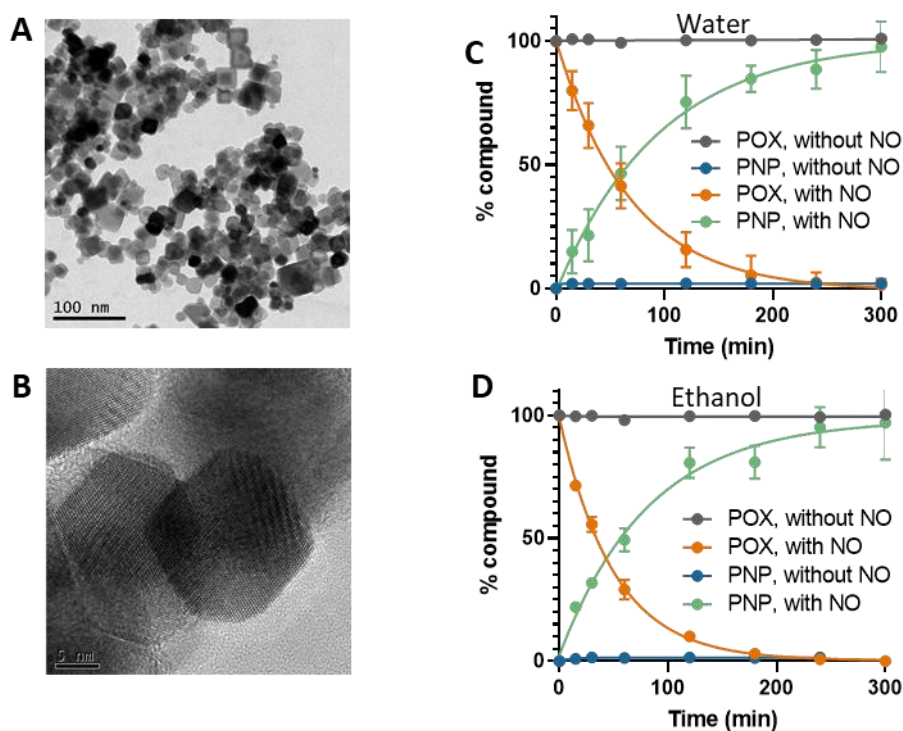
331 Ratio 1 corresponds to total amount of POX recovered at the surface (S) and into the skin (stratum
332 corneum (SC)+ epidermis (E) + dermis (D)+ AM (acceptor medium)) for the control comparatively to
333 the decontaminant system. Ratio 2 corresponds to the same ratio for the percentage of POX absorbed
334 into the skin (SC+E+D+AM). Ratio 3 corresponds to the ratio for the percentage of POX accumulated in
335 the viable skin (E+D+AM).

336 3 RESULTS

337 3.1 NO CeO₂ PARTICLES SYNTHESIS AND CHARACTERIZATION

338 Synthesis of CeO₂ nano-octahedra (NO) was performed as described in part 3.2.1 and in previous
339 publication via a solvothermal pathway [26]. NO characteristics are shown in Figure 1 and in Table 3
340 and 4. Small nanoparticles (6-37 nm) with {111} facets were obtained. Their potential for the
341 degradation of organophosphorus (OPs) was evaluated in this study using paraoxon (POX). This
342 compound has physicochemical properties and chemical functions similar to VX but is less toxic and
343 has been shown to be an interesting simulant [41], [42], [43]. Degradation of POX with or without NO
344 was studied in water and ethanol, the solvents used in the formulation of the peel-off gel. Fit of the

345 data by a pseudo-first order decay model for POX without nanoparticles was not possible as almost no
 346 degradation was detected in 5 h. The degradation of POX increased in the presence of NO particles. As
 347 expected, an increase in para-nitrophenol (PNP), one of the POX degradation products, was detected.
 348 These results demonstrate the interest of using such nanoparticles for decontamination purposes.



349
 350 **Figure 1: NO CeO₂ particles.** A) TEM image. B) HRTEM image. C) Degradation of POX in aqueous solution without or with NO.
 351 D) Degradation of POX in ethanol solution without or with NO. Results are expressed as the quantity of POX or PNP recovered
 352 expressed as % of the initial number of mol of POX added (n=3-5, representation of mean ± SD).

353
 354 **Table 3 : NO CeO₂ particles characterizations.**

Crystal faces	d _{MET} (nm)	S _{BET} (m ² .g ⁻¹)	V _{pores} (cm ³ .g ⁻¹)	Mean pore diameter (nm)
{111}	6-37	60.3	0,1704	11,306

355
 356

357 **Table 4 : Degradation of POX with NO.** Parameters extracted from the kinetic models of degradation of paraoxon with NO
358 CeO₂ particles. *k* is the rate constant *t*_{1/2} the half-life of POX in solution and *R*² is the reliability factor of the pseudo-first order
359 decay function used for the modeling of the degradation.

pH	Water	EtOH
<i>k</i> (min ⁻¹)	0.015	0.020
<i>t</i> _{1/2} (min)	48	34
<i>R</i> ²	0.973	0.997

360

361 3.2 PEELABLE GEL FORMULATION AND CHARACTERIZATION

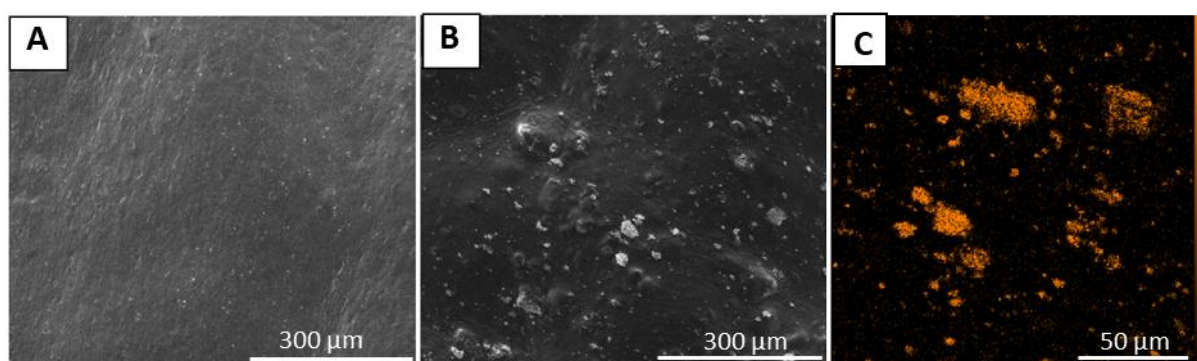
362 Formulation was firstly based on a peelable gel called DDgel, primarily developed by Cao *et al.* and
363 [15], [44], [45] and then optimized. DDgel is a soft jelly-like material, which can dry on the skin in few
364 minutes after application and, can then be peeled off. It has shown great skin decontamination
365 efficiency in removing and back-extracting topically applied chemicals such as chemical warfare
366 simulants and other model chemicals. DDgel contains bentonite (0.5g) and Fuller's earth (2.5 g) which
367 have high adsorption abilities and can therefore adsorb and remove toxic chemicals from skin surface.
368 However, they do not present any degradation properties towards toxics. In the present study,
369 powders were replaced by NO particles to provide degradation properties towards toxics to the
370 formulation. The other components of DDgel are Lutrol F127 (1 g), carboxymethylcellulose
371 (MW = 90 kDa, 0.3 g), water (2 mL) and ethanol (10 mL). The formulation also contains Kollidon® SR
372 (3 g), a physical mixture of lipophilic polyvinyl acetate (PVAc) and more hydrophilic povidone (PVP).

373 3.2.1 Preliminary results

374 Peelable-gels are generally prepared by adding film forming agents (as Kollidon® SR and cellulose in
375 DDgel), thickeners (as cellulose and poloxamer 407 in DDgel) to volatile solvent (as ethanol in DDgel).
376 In a first step of the study, different tests were carried out to optimize the choice of excipients
377 (thickeners, film forming agents, NO particles,...) in the formulation giving a final product with
378 appropriate properties for use as a skin decontamination product: presence of NO particles, stability
379 at room temperature (no visible sedimentation of NO), easy spreading of the formulation on the skin,
380 drying of the gel in few minutes leading to a film easy to peel-off. All formulations were characterized

381 before drying in order to determine their properties in terms of texture, stability, and drying time. The
382 texture analyzer measurements and rheology studies were performed to link sensory parameters and
383 physicochemical properties.

384 When possible, the film obtained after drying of the formulation was characterized by texture analysis
385 and SEM. SEM images were recorded to determine if the repartition of the NO particles was
386 homogenous or not. EDX analysis was also performed to confirm the presence of Ce atoms. As can be
387 seen in Figure 2, the particles are distributed on the whole gel even if aggregates of about 50 nm in
388 size are visible.



389
390 **Figure 2: Microscopy analysis of the film obtained after the gel has dried. A) SEM images of formulation without particles.**
391 **B) SEM images of formulation with particles. C) EDX mapping of a film containing ceria nanoparticles (orange color = cerium**
392 **atoms).**

393
394 Addition of NO particles to the formulation (instead of Fuller's earth and bentonite) tends to make the
395 mixture sticky and elastic and therefore difficult to apply. Several NO quantities were tested (from
396 0.1 g to 3 g) but, a sedimentation was noticeable after few minutes for the highest amount of NO.
397 Thus, an intermediate quantity (1 g) was chosen to maintain the stability of the mixture, while ensuring
398 the degradation properties of the gel provided by the presence of NO particles.

399 Various cellulose derivatives were selected and tested at different molecular weights (carboxymethyl
400 cellulose, CMC and hydroxypropyl cellulose, HPC). It appeared that the most stable gel was obtained
401 with hydroxypropyl cellulose (HPC, MW = 1150 kDa). The high HPC molecular weight combined to its

402 role as a thickener and film-former allowed for better stabilization of the nanoparticles in the mixture.
403 Actually, among cellulose derivatives, HPC appears as the most suitable because it has a good solubility
404 in water and many organic solvents such as ethanol. The highest molecular weight (1 150 kDa) gives
405 higher viscosity for lower polymer concentration while HPC with the lower molecular weight (80 kDa)
406 is more suitable in polar solvent. Therefore, two derivatives (HPC 1 150 or 80 kDa) were selected for
407 the optimization of the formulation of the peel-off gel in the following.

408 When Poloxamer 407 (Lutrol F127) was added as a co-thickener, gels with better consistency were
409 obtained (easier spreading of the gel) and it was maintained in the formulation. Poloxamers are usually
410 used for their gelling properties which depends on their molecular weight but also to modulate the
411 viscosity of liquid formulation at lower concentration. Poloxamer 407 can also be used as solubilizer
412 for certain substances or oils.

413 Then, different film-forming agents were tested: pure PVP, PVP-hexadecene copolymer and PVP-
414 eicosene copolymer and Kollidon® SR. The texture obtained were generally unsatisfactory (polymer
415 poorly dispersed in the mixture for example) and the gel did not form a film after drying. Kollidon® SR
416 proved to be the most interesting film-forming agent. This compound is particularly interesting
417 because lipophilic polyvinyl acetate (PVAc) and more hydrophilic povidone (PVP) give to Kollidon® SR
418 binding ability with chemicals either lipophilic or hydrophilic. Besides, water-soluble PVP creates
419 micropores in the framework of the PVA through which water can penetrate the matrix. Finally, it
420 offers flexible and wash resistant benefits. It can also be noted that hydrogel containing PVP and
421 cellulose can be also used as a wound dressing which indicates that the formulation may be
422 appropriate for use on damaged skin [46].

423 To conclude, the compounds chosen in the formulation were: NO (1g), hydroxypropyl cellulose (HPC,
424 1 150 or 80 kDa), poloxamer 407, Kollidon® SR, water and EtOH.

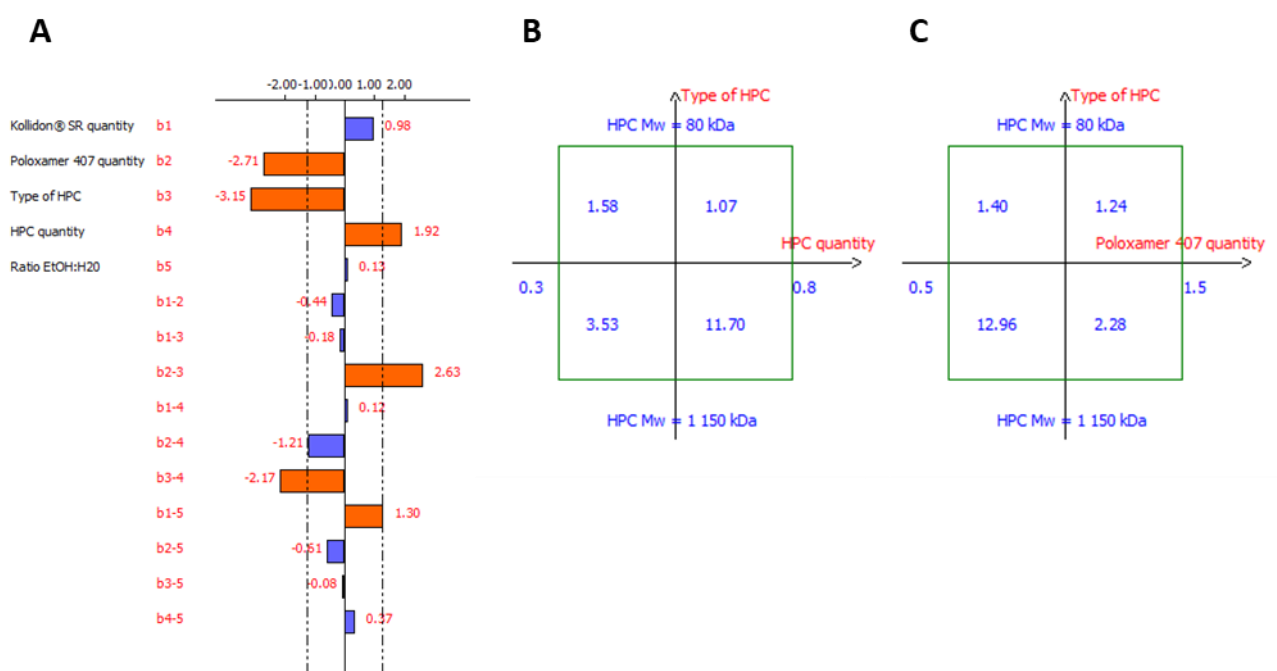
425

426 3.2.2 Design of experiments

427 The results of the design of experiments were very useful to reach the better formulation related to
428 its handling and final properties. Detailed results are presented in the Supplementary Information
429 (Table S1). The gel must be easy to apply but sticky enough to avoid any breaking at skin removal
430 without slowing down the drying process. The results obtained for the gel hardness are presented in
431 Figure 3. The coefficients of Equation 1 are represented as bars with their 95% confidence interval
432 (determined from repeated runs): the bars in orange correspond to statistically significant effects on
433 hardness for 5% risk (Figure 3A). The factors that had the most influence were the amount of
434 poloxamer 407, the type of thickener (HPC of MW = 1 150 kDa or HPW of MW = 80 kDa) and its
435 amount. When the amount of HPC increases from 0.3 g to 0.8 g, the hardness increases by an average
436 of 3.84 N ($b_4=1.92$) which is consistent as HPC acts as a thickening agent. When the lower molecular
437 weight HPC is used (HPC of 80 kDa) instead of the higher one (HPC of 1 150 kDa), the hardness
438 decreases in average of 6.3 N ($b_3=-3.15$) that may be explained by the decrease in the molecular
439 weight. However, when the quantity of poloxamer 407 increases from 0.5 to 1.5 g, the hardness
440 decreases by an average of 5.42 N. Fakhari *et al.* showed that an high addition of ethanol (>25% v/v)
441 to an aqueous solution of poloxamer 407 partially avoided gel formation [47]. Thus, it is likely here that
442 in the near absence of water, the poloxamer 407 did not solvate well. Concerning the two-factor
443 interactions, the most important are X_2X_3 and X_3X_4 . From X_2X_3 representation in Figure 3C, we observed
444 that the effect of the amount of thickening agent on gel hardness depends on the quantity of
445 poloxamer 407 indicating a synergistic effect between both factors. Indeed, if HPC of MW = 1 150 kDa
446 is used, the effect of the quantity of poloxamer 407 on the hardness is very important: a decrease of
447 about 10.68 N is observed when the quantity of poloxamer 407 increases from 0.5 to 1.5g. If HPC of
448 MW = 80 kDa is used, there is no significant effect of the quantity of poloxamer 407 on the hardness
449 (1.4 to 1.24 N). This could be due to poor hydration of the high molecular weight HPC to the benefit of
450 poloxamer 407 under the conditions studied here. Indeed, the presence of water is very low (20 or 1%)
451 in order to allow a quick drying of the formulations. This effect would be less visible for the HPC with

452 a lower molecular weight (80 kDa). Finally, if HPC of MW = 1 150 kDa is used, the effect of the quantity
 453 of HPC on the hardness is very important (Figure 3B): an increase from 3.53 to 11.7 N is observed when
 454 its amount rises from 0.3 to 0.8 g. On the contrary, if HPC with MW = 80 kDa is used, there is no
 455 significant effect of the quantity of HPC on the hardness (1.58 to 1.07 N). The effect of HPC amount
 456 depends on the HPC molecular weight indicating a synergistic effect of both factors.

457 The other DOE responses (Y_2 , Y_3 and Y_4) were exploited as previously described for the gel hardness
 458 (results not shown).



460 **Figure 3: Results of the DOE obtained for the gel hardness. A)** Main effects and two-factor interactions coefficients calculated
 461 for the gel hardness(Y_1). The dotted lines correspond to the 95% confidence interval. **B)** Representation of X_3X_4 .
 462 **C)** Representation of X_2X_3 interactions.

463

464 The percentage of relaxation (Y_2), which is inversely proportional to the elasticity of the product, was
 465 determined. However, among the 16 developed gels, a lot of similar relaxation values were obtained
 466 (13 values above 80%) making the statistical exploitation of the DOE difficult. Nevertheless, several
 467 interesting information can be obtained. Only two formulations (F5 and F7) exhibited very different
 468 elastic behavior with relaxation values below 55% (55 and 43% respectively) when all the other

469 formulations had relaxation values between 70 and 96%. In both cases, a combination of low amounts
470 of Kollidon® SR (2 g) and HPC of MW = 80 kDa (0.3 g) was used indicating that a low molecular weight
471 and low amount of polymer led to a less dense and more elastic network. More generally, the higher
472 the amount of Kollidon® SR, the more the relaxation increases and thus the elasticity decreases. Results
473 also indicate that HPC with high molecular weight (1 150 kDa) promotes an increase of relaxation thus
474 providing less elasticity to the gel compared to HPC with low molecular weight (80 kDa). Moreover,
475 the increase of Kollidon® SR quantity in the formulation enhances the relaxation when HPC with low
476 molecular weight is used, while it has no influence with high molecular weight HPC. Finally a synergistic
477 effect also appears between the ratio EtOH:H₂O and the quantity of poloxamer 407. Gel elasticity
478 increases with the amount of poloxamer 407 with a 99:1 EtOH/H₂O ratio but remained constant for
479 the ratio 80:20. The poor hydration of compounds in the mixture 99:1 may be an explanation of such
480 a phenomenon.

481 Stickiness (Y_3) is correlated to the hardness and the same conclusions were obtained: stickiness is
482 higher if 0.5 g of poloxamer 407 and 0.8 g of high molecular weight HPC are used. For the stability score
483 (Y_4) (at room temperature or 45°C), the main factor influencing the stability is the type of thickening
484 agent (high or low molecular weight HPC), the higher molecular weight giving the better results.
485 Besides a value of 0.5 g of poloxamer 407 improved the stability, probably linked to a decrease of
486 hardness as mentioned previously. Finally, out of all the formulations only 7 of them led to film
487 formation after drying (F1 to F4, F6, F9 and F12) and film flexibility obtained with the texture analyzer
488 were almost all similar (data not shown).

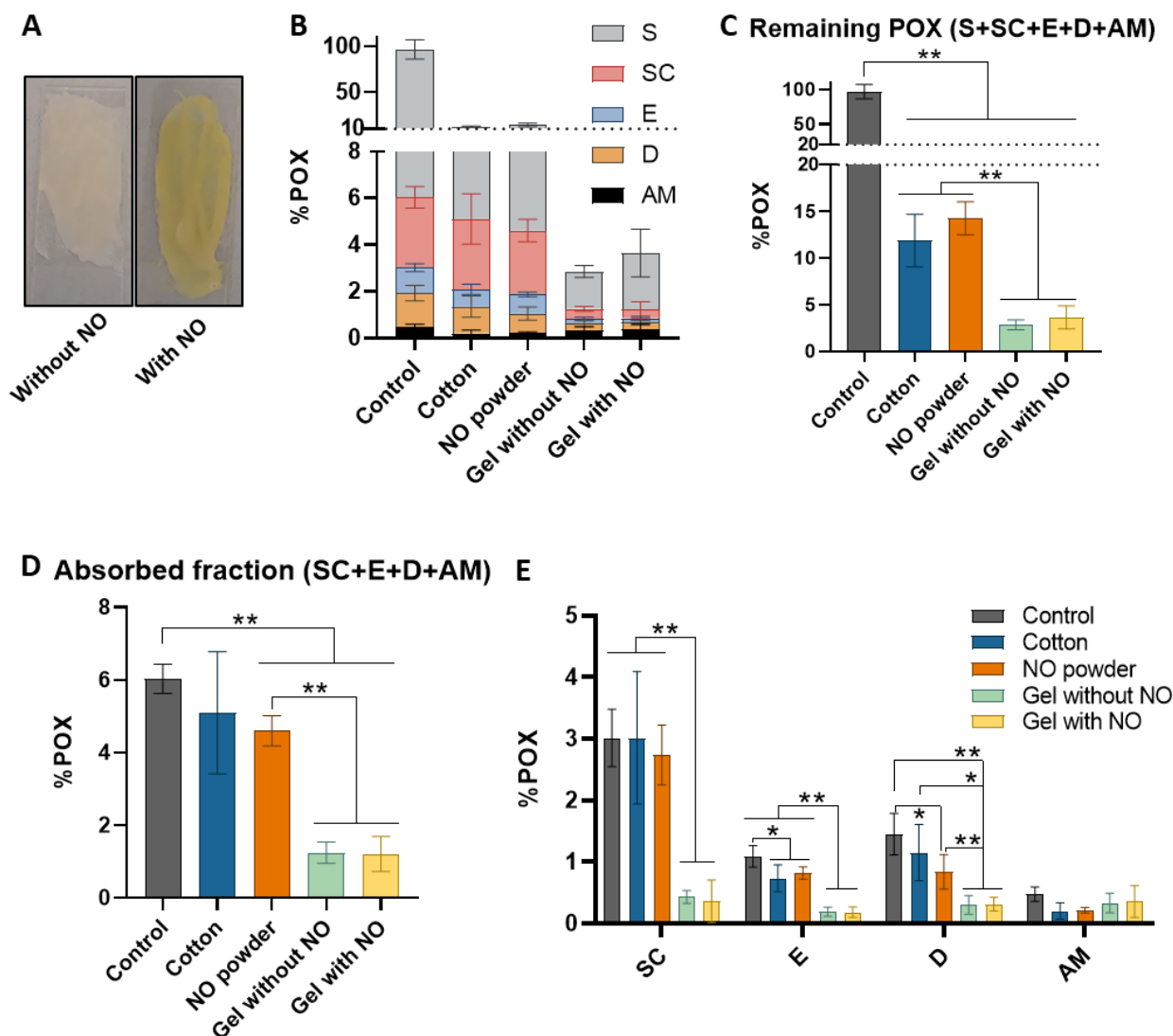
489 Based on these results, the use of high molecular weight HPC appears to be interesting as it brings less
490 elasticity but also a good stability, certainly due to its high molecular weight allowing suspending
491 correctly the particles in the mixture thereby avoiding their sedimentation. Nevertheless, this
492 thickener makes the formulation compact, so a low quantity (0.3 g) should be used to counterbalance
493 this effect. Besides, a small amount of poloxamer 407 (0.5 g), a large amount of Kollidon® SR (3 g) and

494 a EtOH/water 80:20 ratio seem more suitable. Considering all the gel characteristics obtained and
495 regardless of the POX absorption and degradation aspects, F2 formulation (3 g Kollidon® SR, 0.5 g
496 poloxamer 407, 0.3 g of HPC of MW = 1 150 kDa and 80/20 EtOH/water, 1 g of NO) seems to fulfill all
497 the desired criteria for a skin decontamination peelable gel and has been further investigated.

498 3.3 POX DEGRADATION BY THE PEELABLE GEL.

499 In a second step, F2 peelable gels containing NO or not were put into contact with POX. We observed
500 that POX had a good affinity with the gel and penetrated fairly quickly into the formulation. This agrees
501 with observations made by the team of Cao *et al.* who demonstrated extraction of the toxicant from
502 the skin by DDGel [15], [44], [45]. Besides, when POX is mixed into the formulation, a yellow color
503 quickly appears, characteristic of the formation of para-nitrophenol, one POX degradation product as
504 shown Figure 4A. This indicates that NO particles maintain their degradation activities towards POX.
505 This was confirmed by extraction of POX from the gel after 30 min of exposure and quantification by
506 HPLC. $103 \pm 7\%$ of POX was quantified when the gel didn't contain NO CeO₂ particles whereas only 65
507 $\pm 4\%$ was found when the gel did contain NO. In parallel, an increase of PNP is detected with the use
508 of the gel containing NO ($24.3 \pm 14.5\%$) in comparison to the use of the gel without NO ($2.2 \pm 1.3\%$).
509 (Figure S1). These results demonstrate the neutralization ability of the NO-loaded gel.

510 3.4 SKIN DECONTAMINATION EFFICIENCY OF THE PEELABLE GEL INCORPORATING NO



511 **Figure 4: Degradation of POX by the peel-off gel and in vitro decontamination efficiency.** **A)** Picture of the peelable gels
 512 containing NO or not, 30 min after exposure to POX, the yellow color is characteristic of the POX degradation product (PNP).
 513 **B) and C)** Franz cell studies evaluation. Percentage of POX recovered at the surface (S), in the stratum corneum (SC), in the
 514 viable epidermis (E), in the dermis (D) and in the acceptor medium (AM). **D)** Percentage of POX absorbed into the skin at 24h
 515 (quantity recovered in the SC, E, D and AM). **E)** Percentage of POX recovered in the different compartments of the skin at 24h.
 516 Representation of the mean \pm SD, n = 5. Significant differences are indicated, Mann-Whitney test (*: p < 0.05 ; **: p < 0.01).
 517

518

519 Skin decontamination efficiency was evaluated by the Franz cell experiments using pig-ear skin as it
 520 was shown to be relevant model to predict the human skin permeability [48]. The POX applied dose
 521 was 13 mg/cm² (or 10 μ L/cm²) and allowed a full skin coverage. This dose corresponds to severe skin
 522 contamination and also to the one recommended in the AFNOR NF X 52 122 standard. 30 min after
 523 contamination of the skin with POX, decontamination systems were applied. This time point was

524 chosen as it corresponds to a late decontamination procedure, realistic in real use condition. The total
 525 quantity of POX recovered during the different step of the experiment, POX remaining at the surface
 526 (S), in the stratum corneum (SC), in the viable epidermis (E), in the dermis (D) and in the acceptor
 527 medium (AM) was quantified. The non-absorbed fraction (total quantity of chemical present on the
 528 skin surface, S) is the fraction considered as the removable amount from the skin surface. On the other
 529 hand, the absorbed fraction (i.e., sum of the quantities from the SC to R) is the quantity of chemical
 530 that can potentially move into the blood. The skin decontamination results are reported in Figure 4B-
 531 E, Table 5 and Figure S2.

532

533 *Table 5: In vitro distribution of POX through pig-ear full thickness unclipped skin 24 h after an exposure to POX with a*
 534 *decontamination at 30 min using cotton, NO as powder, gel without NO and gel with NO. Results are expressed as % of the*
 535 *POX applied dose (means \pm SD, n = 5). Ratio 1 represents the reduction of the fraction of POX in (S+SC+E+D+AM) in comparison*
 536 *to control, Ratio 2 represents the reduction of the fraction of POX absorbed into the skin (SC+E+D+AM) in comparison to*
 537 *control, Ratio 3 represents the reduction of the fraction of POX in the viable skin (E+D+AM) in comparison to control.*
 538 *R = %control / %sample.*

	Control	Cotton	NO powder	Gel without NO	Gel with NO
Total quantity of POX recovered	96.64 \pm 10.28	92.00 \pm 5.84	67.16 \pm 9.54	92.69 \pm 7.92	61.17 \pm 12.84
Skin surface (S)	90.60 \pm 10.42	6.77 \pm 1.23	9.67 \pm 2.04	1.60 \pm 0.26	2.44 \pm 1.02
Stratum Corneum (SC)	3.02 \pm 0.47	3.02 \pm 1.08	2.74 \pm 0.49	0.43 \pm 0.10	0.36 \pm 0.34
Viable epidermis (E)	1.09 \pm 0.17	0.73 \pm 0.22	0.82 \pm 0.10	0.19 \pm 0.07	0.18 \pm 0.09
Dermis (D)	1.45 \pm 0.34	1.15 \pm 0.46	0.84 \pm 0.28	0.30 \pm 0.15	0.31 \pm 0.11
Acceptor medium (AM)	0.48 \pm 0.12	0.20 \pm 0.13	0.21 \pm 0.05	0.33 \pm 0.16	0.36 \pm 0.26
Absorbed fraction	6.04 \pm 0.40	5.10 \pm 1.68	4.61 \pm 0.42	1.25 \pm 0.29	1.21 \pm 0.48
Ratio 1	-	8.14	6.77	26.46	33.90
Ratio 2	-	1.18	1.31	4.98	4.82
Ratio 3	-	1.45	1.61	3.55	3.68

539

540 The total amount of POX recovered (Figure S2A and Table 5) was over 85% for systems without NO
 541 (control, cotton, gel without NO). It was 67.16% and 61.17% for NO powder and gel with NO
 542 respectively, which clearly indicates the capacity for POX degradation by the particles and is in line

543 with what was observed in the paragraph 3.3. As can be seen in the Figure 4B, the amount of POX in
544 the different skin compartments was different depending on the decontamination method used. The
545 total POX amount recovered after 24 h on the surface and in the skin (S + SC+ E + D + AM) was in all
546 cases, lower for decontaminant systems compared to the control (Figure 4C). For cotton and NO
547 powder about 7-8 times less POX was recovered after 24 hours compared to the control ($p<0.01$) in
548 and onto the skin and 26-34 times less for gels containing or not the NO particles ($p<0.01$) (ratio R1).
549 Gels were statistically always more efficient than other decontamination systems ($p<0.01$). These
550 results demonstrate their higher efficiency for adsorbing and eliminating the toxic from the skin. No
551 significant difference was detected between NO powder and cotton but it should be noted that the
552 quantities of powder used in this study are relatively small and did not allow a total coverage of the
553 skin surface, which probably limited their effectiveness. We can assume that an increase in the amount
554 of NO powder would reduce the amount of POX remaining related to the adsorption and degradation
555 capacities of NO towards the toxicant.

556 Regarding the amount of toxicant absorbed into the skin (SC+E+D+AM, Figure 4D), a significant
557 difference ($p<0.01$) was observed for the treatment with NO powder compared to control, which was
558 not the case for cotton decontamination alone, demonstrating the interest of CeO₂ nanoparticles.
559 Moreover, the efficiency and the interest of the gels was clearly demonstrated with a decrease by
560 about 5 of the quantity of POX absorbed into the skin ($p<0.01$). The same observation was noticed for
561 the viable skin (E+D+AM) with a 3 to 4-fold decrease in the quantity of POX when gels were used in
562 comparison to the control ($p<0.01$).

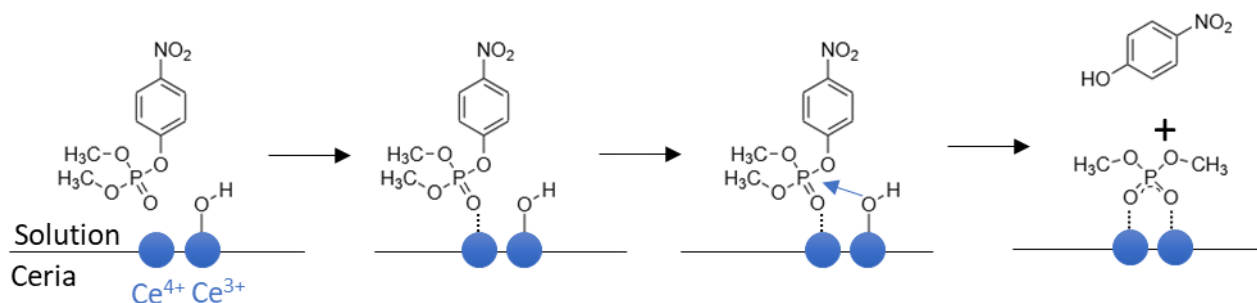
563 Looking more deeply at the distribution of POX in the different layers of the skin (Figure 4E), it can be
564 noted that POX was mainly distributed in the stratum corneum and the gels greatly reduced the
565 amount of POX found in this compartment ($p<0.01$). Similarly, they allowed decreasing the quantity of
566 POX in the viable epidermis and dermis ($p<0.01$).

567 4 DISCUSSION

568 Over the last decade, concern about the chemical warfare agents threat has increased due to several
569 reported attacks as an assassination through the use of VX in Kuala Lumpur in 2017, a murder attempt
570 with nerve agent (“Novichok”) in the United-Kingdom in 2018 and the use of toxics reported several
571 times during the Syrian conflict [1]. Therefore, the development of efficient decontamination systems,
572 especially for skin, and their evaluation has become crucial. To limit the use of war gases in the
573 laboratory many chemicals have been used as simulants [27], [42], [43], [49], [50], [51], [52]. In the
574 case of VX, paraoxon has been identified in the literature [43] and used in this study. It presents
575 physicochemical properties and chemical functions similar to VX and is easily detected thanks to the
576 benzene ring. It is a lipophilic substance which therefore tends to be stored in the upper layers of the
577 skin. It has been used as a simulant because of its molecular weight and logP close to those of VX (275.2
578 $\text{g}\cdot\text{mol}^{-1}$ against 267.4 $\text{g}\cdot\text{mol}^{-1}$ and logP = 1.8 against 2.09 respectively for POX an VX). However, it should
579 be noted that VX penetrates faster and earlier (lower lag time) than POX into the skin. The skin
580 penetration rate on pig skin is 15 times faster for VX than POX [43].

581 In the context of toxic chemicals degradation, several studies have shown the interest of metallic
582 nanoparticles and especially cerium oxide nanoparticles [27], [29], [30], [31]. CeO_2 is from a group of
583 lanthanoids with fluorite type structure and present various application in catalysis, fuels cells, solar
584 cells, pharmacy and medicine. Its catalytic activity towards the hydrolysis of various types of
585 organophosphates (pesticides plasticizers and biologically active molecules) has been studied [53].
586 Different methods have been described in the literature to prepare CeO_2 nanoparticles [25], [26], [27],
587 [30]. In this study, the hydrothermal method has been chosen as it enables large quantities of particles
588 to be obtained quickly and efficiently. In addition, synthesis parameters can be optimized to obtain
589 particles with controlled properties (size, morphology, etc.) [25], [26]. The degradation properties of
590 CeO_2 nanoparticles depends on various factors. Recently, we have demonstrated the influence of CeO_2
591 NPs size, morphology and crystallographic planes on the degradation of paraoxon, with a higher

592 activity of the {111} facets as compared to the {100} facets, or ill-defined surfaces [25]. When an
 593 annealing step is performed after synthesis, the degradation activity is mainly driven by the specific
 594 surface area and the shape of particles appears as a second order effect [26]. In these two studies,
 595 nano-octaedra ceria nanoparticles (NO), which are those used in the present study, have appeared
 596 really interesting for the degradation of POX in aqueous solution. Other factors have been shown to
 597 have an effect on the ceria properties as the ratio of Ce^{3+} and Ce^{4+} , number of hydroxyl groups at the
 598 surface, surface defects abundance [25], [26], [31], [53]. A mechanism has been proposed to explain
 599 the hydrolysis properties of CeO_2 towards OPs and is represented in the Figure 5 [31]. First, a
 600 coordination takes place between a phosphate group and a Ce^{4+} cation followed by a nucleophilic
 601 attack by the Ce^{3+} activated hydroxyl group on the phosphorus atom. The unique redox switching
 602 ability of cerium cations, combined with the high mobility of oxygen in the cerium oxide lattice would
 603 facilitates the dynamic creation and regeneration of this particular spatial arrangement on the cerium
 604 oxide surface (Ce^{3+} , Ce^{4+} , OH group).



605

606 *Figure 5: Degradation of POX to PNP by the CeO_2 surface.*

607

608 As any powder, cerium oxide particles must be formulated to allow an easy decontamination of the
 609 skin and to avoid the spreading or inhalation of the toxicant-loaded particles after decontamination.
 610 In addition, nanoparticles in powder form are very difficult to remove from the skin after application,
 611 and thorough washing of the skin is required to remove them, resulting in high waste production. Few
 612 systems based on cerium oxide nanoparticles for skin decontamination purposes have been

613 formulated. We have previously evaluated the skin decontamination efficiency of CeO₂ nanoparticles
614 as powder or suspension containing 10 wt% CeO₂ and 1 wt% of Guar gum to prevent nanoparticles
615 sedimentation. Suspension have been almost 10 times more efficient than powder regarding the
616 decrease of POX absorption into the skin [27]. Zenerino *et al.* have also developed new topical skin
617 protectants [37] containing ceria nanoparticles and compared an oil in water emulsion and a
618 suspension of a fluorinated thickening polymer (HASE-F) grafted with these NPs. Both skin protectants
619 have decreased the penetration of POX by 3 to 4-fold factors when they have been applied onto the
620 skin before contamination. Bignon *et al.* have also worked on a barrier cream based on CeO₂
621 nanoparticles [38]. They have demonstrated, that the efficiency of the topical skin protectants is due
622 to the presence of ceria particles and depends on their quantity in the formulation as well as their
623 grafting onto a perfluorocarbon thickening polymer and, finally the formulation of the new grafted
624 polymer. These last two formulation are topical skin protectants and therefore destined to be applied
625 on the skin before the contamination on the contrary to the formulation developed in this paper
626 designed to remove the toxic from the skin after decontamination.

627 The choice of the CeO₂ formulation type for skin decontamination purpose is not straightforward as
628 they are often unstable (sedimentation for suspension, possible coalescence for emulsion, syneresis
629 for gels). The goal of this study has been to develop a new system containing CeO₂ nanoparticles but a
630 limited amount of water to avoid a “wash-in” effect, easy to apply and to remove from the skin, able
631 to absorb the toxic agent and to degrade it. Our work has been inspired by the work of Cao *et al.*, and
632 their work on an efficient peelable gel, the DDgel [15], [44], [45]. Cao *et al.* have demonstrated through
633 *in vitro* skin decontamination experiment that DDGel can simultaneously clean chemical contaminant
634 from the skin surface, back-extract toxicant from SC, decrease the quantity of contaminant available
635 for penetrating into the skin and reduce chemical penetration and subsequent systemic absorption. It
636 is interesting to note that DDGel did not peel off SC layers but back- extracted chemicals from SC as
637 demonstrated on different chemical warfare agent simulants for OPs and blistering agents [15], [45].
638 In their studies, Cao *et al.* have found that the percentage of chemicals absorbed into the skin

639 (SC+E+D+AM) and viable skin (E+D+AM) ranged between 2.7 and 6 % and between 2 and 5.5%
640 respectively. This corresponds to a decrease of 4.5 to 12-fold in comparison to non-decontaminated
641 skins [15], [45]. In order to improve the formulation and provides degradation properties, CeO₂
642 nanoparticles have been incorporated and the formulation has then been optimized in this study. The
643 challenge has been to maintain POX access to the CeO₂ nanoparticles entrapped in the gel matrix for
644 efficient degradation of POX. The *in vitro* results have demonstrated that the gel itself was indeed no
645 obstacle to the access of POX to the surface of CeO₂ nanoparticles and maintained their ability to
646 degrade it into safer by-products. In our study, the efficiency of the optimized peel-off gel has been
647 clearly demonstrated with a percentage of POX absorbed into the skin (SC+E+D+AM) and viable skin
648 (E+D+AM) decreasing from 6% of the applied dose without decontamination to 1.21% and 0.85%
649 respectively with the peel-off gel. This corresponds to a decrease by about 5-fold of the quantity of
650 POX absorbed into the skin (SC+E+D+AM) and a decrease of 3.5-fold in the viable skin (E+D+AM) in
651 comparison to non-decontaminated skins, which is much more than the use of cotton or nanoparticles
652 as powder. It can also be noted that the gel without NO particles has been effective in removing the
653 toxicant but has not degraded it. These results are consistent with the results of Cao *et al* described
654 above.

655 In the case of the CeO₂-based peel-off gels developed in this study, the decontamination occurs due
656 to physical interactions or chemical neutralization. Concerning physical interactions, bringing the toxic
657 compound into contact with the gel on the skin enables the toxic compound to be absorbed into the
658 formulation. Depending on the compound, hydrophilic or hydrophobic interactions can take place into
659 the gel, related to the presence of Kollidon SR (a physical mixture of lipophilic polyvinyl acetate (PVAc)
660 and more hydrophilic povidone (PVP) as presented in section 3.2). The gel can then be dried on the
661 skin by evaporation of ethanol, leading to a toxicant-retaining film. This film can then be peeled off,
662 thus retaining the toxicant and facilitating waste removal. It should also be noted that Cao and his
663 team have shown that DDgel, with a formulation very similar to the one developed here, can not only
664 remove the toxicant from the skin surface, but can also back-extract the toxicant from the SC. This is

665 due to the similar or higher partition coefficient of each simulant for the gel than for SC [45]. As their
666 formulation is close to the one developed in this paper, the same mechanism is likely to occur. The
667 efficacy of the gel, thanks to the physical interactions between the gel and the toxicant, is
668 demonstrated in our study. Actually, a very good skin decontamination efficacy for the gel without
669 nanoparticles is observed. Moreover, in the case of the CeO₂-based formulation developed in this
670 study, chemical neutralization can take place. Once the POX has been absorbed into the formulation,
671 it comes into contact with the NO particles, which degrade it into the less toxic by-product PNP
672 (illustrated on Figure S1). The effectiveness of our formula stems from the physical and chemical
673 interactions between the gel and the toxic substance.

674 To finish, CeO₂ on one hand and DDgel on the other have already been shown to be effective for skin
675 decontamination of several chemicals. Therefore, it can be expected that the CeO₂-based formulation
676 prepared in this research will be efficient against various compounds as OPs and blistering agents
677 which should be validated in future studies.

678 5 CONCLUSION

679 Skin contamination with toxic agents remains a great concern and new decontamination systems able
680 to eliminate the toxic from the skin and to degrade it need to be developed and evaluated. Cerium
681 oxide nanoparticles appear promising in this context because of their catalysis properties resulting
682 from their abundant surface defects, large number of surface hydroxyl groups and low redox potential
683 between Ce³⁺ and Ce⁴⁺ cations. To take full advantage of the degradation potential of CeO₂ toward
684 toxic agents, these nanoparticles must be formulated in an appropriate system. In this study, they have
685 been incorporated into a gel that can easily be applied on the skin. This formulation is easier to handle
686 than powder or liquid formulation and avoid dispersion or cross contamination. After application, the
687 gel can quickly dry to form a strippable film. *In vitro* studies have demonstrated the efficiency of such
688 formulation for skin decontamination and its potential to reduce local and systemic absorption, and

689 decrease chemical toxicity. As CeO₂ and the gel are known to be efficient against various toxic, the
690 potential of the formulation developed in this study should be evaluated on other compounds.

691 CREDIT AUTHORSHIP CONTRIBUTION STATEMENT

692 Eloise Thomas: Funding acquisition, Resources, Conceptualization, Methodology, Investigation,
693 Validation, Formal analysis, Supervision, Writing - original draft, Writing – review & editing,
694 Visualization, Project administration.

695 Claire Bordes: Formal analysis, Methodology, Writing - original draft, Writing – review & editing

696 Frédéric Chaput: Resources, Methodology, Investigation, Writing – review & editing.

697 Delphine Arquier: Investigation, Methodology.

698 Stéphanie Briançon: Resources, Conceptualization, Methodology, Writing – review & editing

699 Marie-Alexandrine Bolzinger: Resources, Conceptualization; Methodology, Writing – review & editing.

700

701 DECLARATION OF COMPETING INTEREST

702 The authors declare that they have no known competing financial interests or personal relationships
703 that could have appeared to influence the work reported in this paper.

704

705 ACKNOWLEDGMENTS

706 We thank Clara Haïtaian for her help of some gel formulations. We thank the Coslife platform for the
707 equipments used in the project. This work was funded by the Université Claude Bernard Lyon 1.

708 For the purpose of Open Access, a CC-BY public copyright licence has been applied by the authors to
709 the present document and will be applied to all subsequent versions up to the Author Accepted
710 Manuscript arising from this submission.

711 REFERENCES

-
- 712 [1] B. Picard, I. Chataigner, J. Maddaluno, et J. Legros, « Introduction to chemical warfare agents,
713 relevant simulants and modern neutralisation methods », *Organic & Biomolecular Chemistry*, vol.
714 17, n° 27, p. 6528-6537, 2019, doi: 10.1039/C9OB00802K.
- 715 [2] S. Chauhan *et al.*, « Chemical warfare agents », *Environ. Toxicol. Pharmacol.*, vol. 26, n° 2, p.
716 113-122, sept. 2008, doi: 10.1016/j.etap.2008.03.003.
- 717 [3] M. S. Tudosie *et al.*, « The Synthesis and Toxicological Characterization of Neurotoxic Chemical
718 Agents Simulants », *Rev. Chim.*, vol. 70, n° 11, p. 3881-3888, déc. 2019, doi:
719 10.37358/RC.19.11.7664.
- 720 [4] M. D. Schwartz, C. G. Hurst, M. A. Kirk, S. J.D. Reedy, et E. H. Braue, « Reactive Skin
721 Decontamination Lotion (RSDL) for the Decontamination of Chemical Warfare Agent (CWA)
722 Dermal Exposure », *Current Pharmaceutical Biotechnology*, vol. 13, n° 10, p. 1971-1979, août
723 2012, doi: 10.2174/138920112802273191.
- 724 [5] H. P. Chan, H. Zhai, X. Hui, et H. I. Maibach, « Skin decontamination: principles and perspectives »,
725 *Toxicol Ind Health*, vol. 29, n° 10, p. 955-968, nov. 2013, doi: 10.1177/0748233712448112.
- 726 [6] N. Kashetsky, R. M. Law, et H. I. Maibach, « Efficacy of water skin decontamination in vivo in
727 humans: A systematic review », *Journal of Applied Toxicology*, vol. 42, n° 3, p. 346-359, 2022, doi:
728 10.1002/jat.4230.
- 729 [7] L. Thors, E. Wigenstam, J. Qvarnström, L. Hägglund, et A. Bucht, « Improved skin
730 decontamination efficacy for the nerve agent VX », *Chemico-Biological Interactions*, vol. 325, p.
731 109135, juill. 2020, doi: 10.1016/j.cbi.2020.109135.
- 732 [8] R. P. Moody et H. I. Maibach, « Skin decontamination: Importance of the wash-in effect », *Food
733 and Chemical Toxicology*, vol. 44, n° 11, p. 1783-1788, nov. 2006, doi: 10.1016/j.fct.2006.05.020.
- 734 [9] T. James, L. Izon-Cooper, S. Collins, H. Cole, et T. Marczylo, « The wash-in effect and its
735 significance for mass casualty decontamination », *Journal of Toxicology and Environmental
736 Health, Part B*, vol. 25, n° 3, p. 113-134, avr. 2022, doi: 10.1080/10937404.2022.2042443.
- 737 [10] H. Zhu, E.-C. Jung, C. Phuong, X. Hui, et H. Maibach, « Effects of soap–water wash on human
738 epidermal penetration », *Journal of Applied Toxicology*, vol. 36, n° 8, p. 997-1002, 2016, doi:
739 10.1002/jat.3258.
- 740 [11] L. Thors, M. Koch, E. Wigenstam, B. Koch, L. Hägglund, et A. Bucht, « Comparison of skin
741 decontamination efficacy of commercial decontamination products following exposure to VX on
742 human skin », *Chemico-Biological Interactions*, vol. 273, p. 82-89, août 2017, doi:
743 10.1016/j.cbi.2017.06.002.
- 744 [12] H. Matar, S. C. Price, et R. P. Chilcott, « Further studies of the efficacy of military, commercial and
745 novel skin decontaminants against the chemical warfare agents sulphur Mustard, Soman and
746 VX », *Toxicology in Vitro*, vol. 54, p. 263-268, févr. 2019, doi: 10.1016/j.tiv.2018.10.008.
- 747 [13] H. Matar, A. Guerreiro, S. A. Piletsky, S. C. Price, et R. P. Chilcott, « Preliminary evaluation of
748 military, commercial and novel skin decontamination products against a chemical warfare agent
749 simulant (methyl salicylate) », *Cutan Ocul Toxicol*, vol. 35, n° 2, p. 137-144, 2016, doi:
750 10.3109/15569527.2015.1072544.

- 751 [14] P. Rolland, M.-A. Bolzinger, C. Cruz, D. Josse, et S. Briançon, « Hairy skin exposure to VX in vitro:
752 Effectiveness of delayed decontamination », *Toxicology in Vitro*, vol. 27, n° 1, p. 358-366, févr.
753 2013, doi: 10.1016/j.tiv.2012.08.014.
- 754 [15] Y. Cao, X. Hui, H. Zhu, A. Elmahdy, et H. Maibach, « In vitro human skin permeation and
755 decontamination of 2-chloroethyl ethyl sulfide (CEES) using Dermal Decontamination Gel
756 (DDGel) and Reactive Skin Decontamination Lotion (RSDL) », *Toxicology Letters*, vol. 291, p.
757 86-91, juill. 2018, doi: 10.1016/j.toxlet.2018.04.015.
- 758 [16] E. H. Braue, K. H. Smith, B. F. Doxzon, H. L. Lumpkin, et E. D. Clarkson, « Efficacy studies of
759 Reactive Skin Decontamination Lotion, M291 Skin Decontamination Kit, 0.5% bleach, 1% soapy
760 water, and Skin Exposure Reduction Paste Against Chemical Warfare Agents, Part 2: Guinea pigs
761 challenged with soman », *Cutaneous and Ocular Toxicology*, vol. 30, n° 1, p. 29-37, mars 2011,
762 doi: 10.3109/15569527.2010.515281.
- 763 [17] A. M. Feschuk, R. M. Law, et H. I. Maibach, « A Review of Reactive Skin Decontamination Lotion
764 Efficacy », in *Dermal Absorption and Decontamination: A Comprehensive Guide*, A. M. Feschuk,
765 R. M. Law, et H. I. Maibach, Éd., Cham: Springer International Publishing, 2022, p. 133-145. doi:
766 10.1007/978-3-031-09222-0_8.
- 767 [18] A. M. Feschuk, R. M. Law, et H. I. Maibach, « Comparative efficacy of Reactive Skin
768 Decontamination Lotion (RSDL): A systematic review », *Toxicology Letters*, vol. 349, p. 109-114,
769 oct. 2021, doi: 10.1016/j.toxlet.2021.06.010.
- 770 [19] J. P. Kumar, P. V. R. K. Ramacharyulu, G. K. Prasad, A. R. Srivastava, et B. Singh, « Molecular sieves
771 supported with metal oxide nanoparticles: synthesis, characterization and decontamination of
772 sulfur mustard », *J. Porous Mat.*, vol. 22, n° 1, p. 91-100, févr. 2015, doi: 10.1007/s10934-014-
773 9876-6.
- 774 [20] C. Bisio *et al.*, « Nanosized inorganic metal oxides as heterogeneous catalysts for the degradation
775 of chemical warfare agents », *Catalysis Today*, vol. 277, p. 192-199, nov. 2016, doi:
776 10.1016/j.cattod.2015.12.023.
- 777 [21] G. K. Prasad *et al.*, « Decontamination of Yperite using mesoporous mixed metal oxide
778 nanocrystals », *Journal of Hazardous Materials*, vol. 183, n° 1, p. 847-852, nov. 2010, doi:
779 10.1016/j.jhazmat.2010.07.104.
- 780 [22] A. Kiani et K. Dastafkan, « Zinc oxide nanocubes as a destructive nanoadsorbent for the
781 neutralization chemistry of 2-chloroethyl phenyl sulfide: A sulfur mustard simulant », *Journal of*
782 *Colloid and Interface Science*, vol. 478, p. 271-279, sept. 2016, doi: 10.1016/j.jcis.2016.06.025.
- 783 [23] K. Kim, O. G. Tsay, D. A. Atwood, et D. G. Churchill, « Destruction and Detection of Chemical
784 Warfare Agents », *Chem. Rev.*, vol. 111, n° 9, p. 5345-5403, sept. 2011, doi: 10.1021/cr100193y.
- 785 [24] A. Sellik *et al.*, « Degradation of paraoxon (VX chemical agent simulant) and bacteria by
786 magnesium oxide depends on the crystalline structure of magnesium oxide », *Chem.-Biol.*
787 *Interact.*, vol. 267, p. 67-73, avr. 2017, doi: 10.1016/j.cbi.2016.11.023.
- 788 [25] I. Trenque *et al.*, « Shape-selective synthesis of nanoceria for degradation of paraoxon as a
789 chemical warfare simulant », *Phys. Chem. Chem. Phys.*, vol. 21, n° 10, p. 5455-5465, 2019, doi:
790 10.1039/C9CP00179D.
- 791 [26] I. Trenque *et al.*, « Synthesis routes of CeO₂ nanoparticles dedicated to organophosphorus
792 degradation: a benchmark », *CrystEngComm*, vol. 22, n° 10, p. 1725-1737, 2020, doi:
793 10.1039/C9CE01898K.
- 794 [27] A. Salerno, T. Devers, M.-A. Bolzinger, J. Pelletier, D. Josse, et S. Briançon, « In vitro skin
795 decontamination of the organophosphorus pesticide Paraoxon with nanometric cerium oxide
796 CeO₂ », *Chemico-Biological Interactions*, vol. 267, p. 57-66, avr. 2017, doi:
797 10.1016/j.cbi.2016.04.035.
- 798 [28] A. Salerno, I. Pitault, T. Devers, J. Pelletier, et S. Briançon, « Model-based optimization of
799 parameters for degradation reaction of an organophosphorus pesticide, paraoxon, using CeO₂
800 nanoparticles in water media », *Environmental Toxicology and Pharmacology*, vol. 53, p. 18-28,
801 juill. 2017, doi: 10.1016/j.etap.2017.04.020.

- 802 [29] J. Tolasz *et al.*, « Room-temperature synthesis of nanoceria for degradation of organophosphate
803 pesticides and its regeneration and reuse », *RSC Advances*, vol. 10, n° 24, p. 14441-14450, 2020,
804 doi: 10.1039/D0RA00937G.
- 805 [30] P. Janoš *et al.*, « Cerium oxide for the destruction of chemical warfare agents: A comparison of
806 synthetic routes », *Journal of Hazardous Materials*, vol. 304, p. 259-268, mars 2016, doi:
807 10.1016/j.jhazmat.2015.10.069.
- 808 [31] P. Janoš *et al.*, « Can cerium oxide serve as a phosphodiesterase-mimetic nanozyme? »,
809 *Environmental Science: Nano*, vol. 6, n° 12, p. 3684-3698, 2019, doi: 10.1039/C9EN00815B.
- 810 [32] S. Das, J. M. Dowding, K. E. Klump, J. F. McGinnis, W. Self, et S. Seal, « Cerium oxide nanoparticles:
811 applications and prospects in nanomedicine », *Nanomedicine*, vol. 8, n° 9, p. 1483-1508, sept.
812 2013, doi: 10.2217/nnm.13.133.
- 813 [33] V. Forest, L. Leclerc, J.-F. Hochepped, A. Trouvé, G. Sarry, et J. Pourchez, « Impact of cerium oxide
814 nanoparticles shape on their in vitro cellular toxicity », *Toxicology in Vitro*, vol. 38, p. 136-141,
815 févr. 2017, doi: 10.1016/j.tiv.2016.09.022.
- 816 [34] F. Larese Filon, M. Mauro, G. Adami, M. Bovenzi, et M. Crosera, « Nanoparticles skin absorption:
817 New aspects for a safety profile evaluation », *Regulatory Toxicology and Pharmacology*, vol. 72,
818 n° 2, p. 310-322, juill. 2015, doi: 10.1016/j.yrtph.2015.05.005.
- 819 [35] N. Sharma, M. Chaudhary, B. S. Butola, J. K. Jeyabalaji, D. P. Pathak, et R. K. Sharma,
820 « Preparation, characterization and evaluation of the zinc titanate and silver nitrate incorporated
821 wipes for topical chemical and biological decontamination », *Materials Science and Engineering:
822 C*, vol. 96, p. 183-196, mars 2019, doi: 10.1016/j.msec.2018.10.056.
- 823 [36] S. T. Hobson et H. Braue, « Active topical skin protectants using reactive nanoparticles », US
824 6403653 B1
- 825 [37] A. Zenerino *et al.*, « New CeO₂ nanoparticles-based topical formulations for the skin protection
826 against organophosphates », *Toxicology Reports*, vol. 2, p. 1007-1013, janv. 2015, doi:
827 10.1016/j.toxrep.2015.07.003.
- 828 [38] C. Bignon, S. Amigoni, T. Devers, et F. Guittard, « Barrier cream based on CeO₂ nanoparticles
829 grafted polymer as an active compound against the penetration of organophosphates »,
830 *Chemico-Biological Interactions*, vol. 267, p. 17-24, avr. 2017, doi: 10.1016/j.cbi.2016.03.002.
- 831 [39] L. Bromberg et T. A. Hatton, « Nerve Agent Destruction by Recyclable Catalytic Magnetic
832 Nanoparticles », *Ind. Eng. Chem. Res.*, vol. 44, n° 21, p. 7991-7998, oct. 2005, doi:
833 10.1021/ie0506926.
- 834 [40] G. E. P. Box, J. S. Hunter, et W. G. Hunter, *Statistics for experimenters: design, innovation and
835 discovery*, 2. ed. in Wiley series in probability and statistics. New York: Wiley, 2005.
- 836 [41] A. Salerno, M. A. Bolzinger, P. Rolland, Y. Chevalier, D. Josse, et S. Briançon, « Pickering emulsions
837 for skin decontamination », *Toxicology in Vitro*, vol. 34, p. 45-54, 2016, doi:
838 10.1016/j.tiv.2016.03.005.
- 839 [42] V. Vallet, C. Cruz, D. Josse, A. Bazire, G. Lallement, et I. Boudry, « In vitro percutaneous
840 penetration of organophosphorus compounds using full-thickness and split-thickness pig and
841 human skin », *Toxicology in Vitro*, vol. 21, n° 6, p. 1182-1190, sept. 2007, doi:
842 10.1016/j.tiv.2007.03.007.
- 843 [43] V. Vallet, C. Cruz, J. Licausi, A. Bazire, G. Lallement, et I. Boudry, « Percutaneous penetration and
844 distribution of VX using in vitro pig or human excised skin: Validation of demeton-S-methyl as
845 adequate simulant for VX skin permeation investigations », *Toxicology*, vol. 246, n° 1, p. 73-82,
846 avr. 2008, doi: 10.1016/j.tox.2007.12.027.
- 847 [44] Y. Cao, X. Hui, et H. I. Maibach, « Effect of superabsorbent polymers (SAP) and metal organic
848 frameworks (MOF) wiping sandwich patch on human skin decontamination and detoxification in
849 vitro », *Toxicol Lett*, vol. 337, p. 7-17, févr. 2021, doi: 10.1016/j.toxlet.2020.11.004.
- 850 [45] Y. Cao, A. Elmahdy, H. Zhu, X. Hui, et H. Maibach, « Binding affinity and decontamination of
851 dermal decontamination gel to model chemical warfare agent simulants », *Journal of Applied
852 Toxicology*, vol. 38, n° 5, p. 724-733, 2018, doi: 10.1002/jat.3580.

- 853 [46] N. Roy, N. Saha, T. Kitano, et P. Saha, « Development and Characterization of Novel Medicated
854 Hydrogels for Wound Dressing », *Soft Materials*, vol. 8, n° 2, p. 130-148, juin 2010, doi:
855 10.1080/15394451003756282.
- 856 [47] A. Fakhari, M. Corcoran, et A. Schwarz, « Thermogelling properties of purified poloxamer 407 »,
857 *Heliyon*, vol. 3, n° 8, p. e00390, août 2017, doi: 10.1016/j.heliyon.2017.e00390.
- 858 [48] P. Rolland, M.-A. Bolzinger, C. Cruz, S. Briançon, et D. Josse, « Human scalp permeability to the
859 chemical warfare agent VX », *Toxicology in Vitro*, vol. 25, n° 8, p. 1974-1980, déc. 2011, doi:
860 10.1016/j.tiv.2011.06.021.
- 861 [49] S. F. de A. Cavalcante *et al.*, « Synthesis and in vitro evaluation of neutral aryloximes as
862 reactivators of Electrophorus eel acetylcholinesterase inhibited by NEMP, a VX surrogate »,
863 *Chemico-Biological Interactions*, vol. 309, p. 108682, août 2019, doi: 10.1016/j.cbi.2019.05.048.
- 864 [50] E. C. Meek *et al.*, « Synthesis and In Vitro and In Vivo Inhibition Potencies of Highly Relevant
865 Nerve Agent Surrogates », *Toxicological Sciences*, vol. 126, n° 2, p. 525-533, avr. 2012, doi:
866 10.1093/toxsci/kfs013.
- 867 [51] J. Millerioux *et al.*, « Evaluation of in vitro tests to assess the efficacy of formulations as topical
868 skin protectants against organophosphorus compounds », *Toxicology in Vitro*, vol. 23, n° 1, p.
869 127-133, févr. 2009, doi: 10.1016/j.tiv.2008.09.014.
- 870 [52] T. James *et al.*, « Chemical warfare agent simulants for human volunteer trials of emergency
871 decontamination: A systematic review », *Journal of Applied Toxicology*, vol. 38, n° 1, p. 113-121,
872 2018, doi: <https://doi.org/10.1002/jat.3527>.
- 873 [53] J. Ederer *et al.*, « Nanocrystalline cerium oxide for catalytic degradation of paraoxon methyl:
874 Influence of CeO₂ surface properties », *Journal of Environmental Chemical Engineering*, vol. 9, n°
875 5, p. 106229, oct. 2021, doi: 10.1016/j.jece.2021.106229.
- 876

877

878 FIGURE CAPTIONS

879 **Figure 1: NO CeO₂ particles. A)** TEM image. **B)** HRTEM image. **C)** Degradation of POX in aqueous
880 solution without or with NO. **D)** Degradation of POX in ethanol solution without or with NO. Results
881 are expressed as the quantity of POX or PNP recovered expressed as % of the initial number of mol of
882 POX added (n=3-5, representation of mean ± SD).

883 **Figure 2: Microscopy analysis of the film obtained after the gel has dried. A)** SEM images of
884 formulation without particles. **B)** SEM images of formulation with particles. **C)** EDX mapping of a film
885 containing ceria nanoparticles (orange color = cerium atoms)

886 **Figure 3: Results of the DOE obtained for the gel hardness. A)** Main effects and two-factor
887 interactions coefficients calculated for the gel hardness(Y₁). The dotted lines correspond to the 95%
888 confidence interval. **B)** Representation of X₃X₄. **C)** Representation of X₂X₃ interactions.

889 **Figure 4: Degradation of POX by the peel-off gel and in vitro decontamination efficiency. A)** Picture
890 of the peelable gels containing NO or not, 30 min after exposure to POX, the yellow color is
891 characteristic of the POX degradation product (PNP). **B) and C)** Franz cell studies evaluation.
892 Percentage of POX recovered at the surface (S), in the stratum corneum (SC), in the viable epidermis
893 (E), in the dermis (D) and in the acceptor medium (AM). **D)** Percentage of POX absorbed into the skin
894 at 24h (quantity recovered in the SC, E, D and AM). **E)** Percentage of POX recovered in the different
895 compartments of the skin at 24h. Representation of the mean ± SD, n = 5. Significant difference are
896 indicated, Mann-Whitney test (*: p< 0.05 ; **: p<0.01).

897 **Figure 5: Degradation of POX to PNP by at the CeO₂ surface.**

898

899 **TABLE CAPTIONS**

900 **Table 1: Fixed and variable factors used for the experimental design.**

901 **Table 2: Formulations prepared according to a 2⁵⁻¹ fractional factorial design.**

902 **Table 3: NO CeO₂ particles characterizations.**

903 **Table 6 : Degradation of POX with NO.** Parameters extracted from the kinetic models of degradation
904 of paraoxon with NO CeO₂ particles. k is the rate constant t_{1/2} the half-life of POX in solution and R² is
905 the reliability factor of the pseudo-first order decay function used for the modeling of the degradation.

906 **Table 7: *In vitro* distribution of POX through pig-ear full thickness unclipped skin 24 h after an**
907 **exposure to POX with a decontamination at 30 min** using cotton, NO as powder, gel without NO and
908 gel with NO. Results are expressed as % of the POX applied dose (means ± SD, n = 5). Ratio 1 represents
909 the reduction of the fraction of POX in (S+SC+E+D+AM) in comparison to control, Ratio 2 represents
910 the reduction of the fraction of POX absorbed into the skin (SC+E+D+AM) in comparison to control,
911 Ratio 3 represents the reduction of the fraction of POX in the viable skin (E+D+AM) in comparison to
912 control. R= %control / %sample.

913